

A New Technique to Extract Oxide Trap Time Constants in MOSFET's

Tahui Wang, Senior Member, IEEE, T. E. Chang, L. P. Chiang, and C. Huang

Abstract— A new technique to determine oxide trap time constants in a 0.6 μm n-MOSFET subject to hot electron stress has been proposed. In this method, we used GIDL current as a direct monitor of the oxide charge detrapping-induced transient characteristics. An analytical model relating the GIDL current evolution to oxide trap time constants was derived. Our result shows that under a field-emission dominant oxide charge detrapping condition, $V_{gs} = -4$ V and $V_{ds} = 3$ V, the hot electron stress generated oxide traps exhibit two distinct time constants from seconds to several tens of seconds.

I. INTRODUCTION

TRAP creation in gate oxide due to hot carrier injection has been recognized as a major reliability concern in submicron CMOS and flash EEPROM technologies [1]–[3]. For example, threshold voltage shift, oxide leakage in a floating gate [3] and oxide wearout are all related to oxide trap creation. In the past, physics and characteristics of oxide trap charging/discharging mechanisms have been intensively studied [4]–[9]. The time-dependence of oxide trapped charge was usually monitored by use of flatband voltage as an indicator [4]. This approach is not appropriate for hot carrier stress generated oxide traps in a MOSFET since the traps have a nonuniform spatial distribution along the channel. Moreover, the flatband voltage shift extracted at each measurement time break only gives a discrete and indirect description of a charge trapping/detrapping process. Third, flatband voltage is linearly dependent on oxide charge and thus may not provide sufficient sensitivity to an oxide charge variation. In contrast, it can be shown that a GIDL current arising from band-to-band tunneling in a MOSFET [10] exhibits an exponential dependence on oxide charge. In this letter, a new technique to determine oxide trap time constants from a GIDL current transient was proposed.

A conventional S/D n-MOSFET with 120 Å gate oxide, 0.6 μm gate length, and 20 μm gate width was used. The device was stressed under a maximum gate current (I_g) injection condition, $V_{gs} = 8$ V and $V_{ds} = 5$ V, for 2000 s. It was reported that the maximum I_g stress can generate a large amount of oxide traps while interface trap creation is moderate [11], [12]. A measurement consisting of a series of

oxide trap charging and discharging conditions was performed. During the charge detrapping phase, the evolution of a GIDL current was monitored continuously in time to extract oxide trap time constants.

II. MODEL OF GIDL CURRENT TRANSIENT

Fig. 1 illustrates the energy band diagram of oxide electron detrapping near the Si/SiO₂ surface. A typical GIDL bias condition is applied. A strong oxide field due to a large drain-to-gate bias (V_{dg}) causes electron emission from oxide traps to the conduction band of the n-type drain. As a result of electron detrapping, both the oxide field and silicon surface field decrease and the GIDL current decays with time. The formulation of the electron detrapping induced GIDL current transient is shown below.

Assume the hot electron stress generated oxide traps have N different detrapping time constants. The oxide charge detrapping rate for each kind of oxide traps is

$$\frac{dQ_i}{dt} = -\frac{Q_i}{\tau_i} \quad (1)$$

and

$$Q_i(t) = Q_i(0) \exp(-t/\tau_i) \quad i = 1 \text{ to } N. \quad (2)$$

By applying the Gauss law, the change of the Si surface field ΔF_s due to electron detrapping is

$$\begin{aligned} \Delta F_s &= \sum_{i=1}^N \frac{t_{ox} - d_i}{\epsilon_{si} t_{ox}} \Delta Q_i \\ &= \sum_{i=1}^N \frac{t_{ox} - d_i}{\epsilon_{si} t_{ox}} Q_i(0) [1 - \exp(-t/\tau_i)] \end{aligned} \quad (3)$$

where t_{ox} is the gate oxide thickness and d_i is a distance from the centroid of the traps to the Si/SiO₂ surface. The band-to-band tunneling induced GIDL current, also illustrated in Fig. 1, is expressed below [10]

$$I_d = A F_s \exp(-B/F_s). \quad (4)$$

Assuming ΔF_s is small compared with the initial surface field $F_s(t=0)$ and using Taylor's expansion, (4) is reduced to

$$\begin{aligned} I_d(t) &= A(F_s(0) - \Delta F_s) \exp\left(-\frac{B}{F_s(0) - \Delta F_s}\right) \\ &\simeq A F_s(0) (1 - \Delta F_s/F_s(0)) \exp(-B/F_s(0)) \\ &\quad \cdot \exp\left(-\frac{B}{F_s^2(0)} \Delta F_s\right) \end{aligned}$$

Manuscript received March 18, 1996. This work was supported by the National Science Council, R.O.C., under Contract NSC85-2215-E009-050.

T. Wang, T. E. Chang, and L. P. Chiang are with Department of Electronics Engineering, Institute of Electronics, National Chiao-Tung University, Hsin-Chu, Taiwan, R.O.C.

C. Huang is with Technology Development Dept., Macronix Co., Hsin-Chu, Taiwan, R.O.C.

Publisher Item Identifier S 0741-3106(96)06008-9.

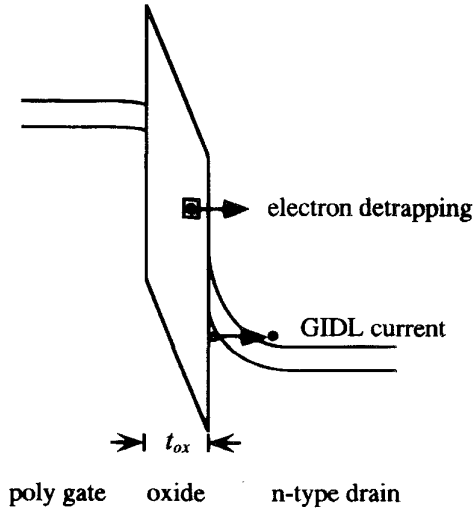


Fig. 1. Schematic representation of the energy band diagram of field-enhanced electron detrapping and band-to-band tunneling induced GIDL current.

$$\simeq I_d(0) \exp\left(-\frac{B}{F_s^2(0)} \Delta F_s\right) \quad (5)$$

and

$$\begin{aligned} \ln(I_d(t)) &= \ln(I_d(0)) - \frac{B}{F_s^2(0)} \Delta F_s \\ &= \ln(I_d(0)) - \sum_{i=1}^N \beta_i [1 - \exp(-t/\tau_i)] \end{aligned} \quad (6)$$

where

$$\beta_i \equiv \frac{B}{F_s^2(0)} \frac{t_{ox} - d_i}{\epsilon_{si} t_{ox}} Q_i(0). \quad (7)$$

It is noteworthy that the GIDL current is very sensitive to oxide charge. It is $\ln(I_d(t))$ in (6) to have an exponential decay with time.

Assuming the transient behavior of the GIDL current is dominated by the i -th kind of the traps in a certain period of time, the following equation can be immediately derived from (6)

$$\ln\left(\left|\frac{d}{dt}[\ln(I_d)]\right|\right) = \ln(\beta_i/\tau_i) - t/\tau_i. \quad (8)$$

Therefore, the oxide trap time constant τ_i can be extracted from the slope of the $\ln\left(\left|\frac{d}{dt}[\ln(I_d)]\right|\right)$ versus time plot.

III. RESULTS AND DISCUSSIONS

Fig. 2 shows the temporal variation of the pre-stress and post-stress drain currents in electron trapping and detrapping phases in the conventional S/D MOSFET. The bias conditions in the trapping and detrapping phases are $V_{gs} = 3.5$ V and $V_{ds} = 3.5$ V, and $V_{gs} = -4$ V and $V_{ds} = 3$ V respectively. In this measurement, the trapping/detrapping cycle repeats two times. No noticeable difference in the drain current between

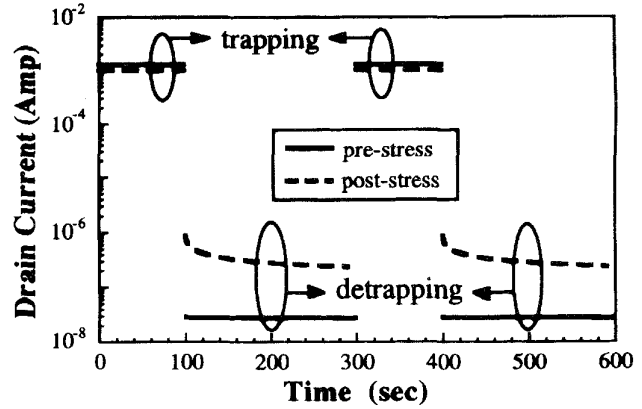


Fig. 2. Temporal variation of pre-stress and post-stress drain currents in electron trapping and detrapping phases. Trapping phase: $V_{gs} = 3.5$ V and $V_{ds} = 3.5$ V. Detrapping phase: $V_{gs} = -4$ V and $V_{ds} = 3$ V.

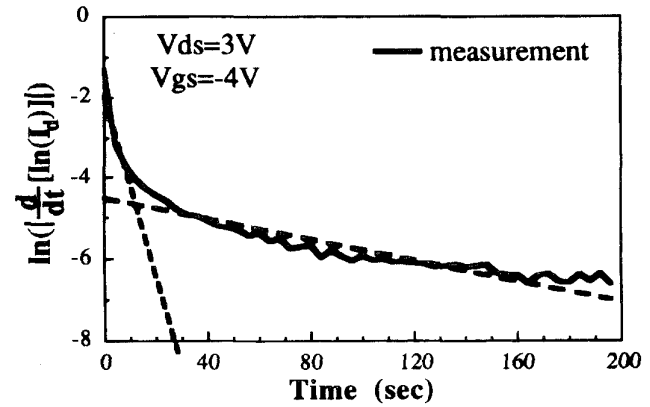


Fig. 3. The plot of $\ln\left(\left|\frac{d}{dt}[\ln(I_d)]\right|\right)$ versus time. The two linear slopes shown by the dashed lines indicate the existence of two oxide charge detrapping times.

the two cycles is observed, which implies no stress effect in the measurement itself. In the electron trapping phase, a small hot electron gate current (about 1pA) was obtained to fill the oxide traps by electron thermal capture. The drain current in the trapping phase declines after stress due to a positive threshold voltage shift resulting from electron occupation of the acceptor-like oxide traps. On the contrary, the post-stress GIDL current in the detrapping phase is greatly enhanced and its transient behavior becomes particularly pronounced. This transient phenomenon can be explained by two possible mechanisms, electron emission from oxide traps or hot hole injection incurred hole-trapped electron recombination. Since a modest V_{ds} of 3 V was applied in the measurement, lateral field enhanced hot hole injection is unlikely to happen. Thus, trapped electron emission via field-enhanced quantum tunneling should be a mechanism responsible for the observed transient. This result is different from the conclusion by Cheng *et al.* at a large V_{dg} [13] that the GIDL current transient is mainly caused by hot hole injection. To study the trap transient

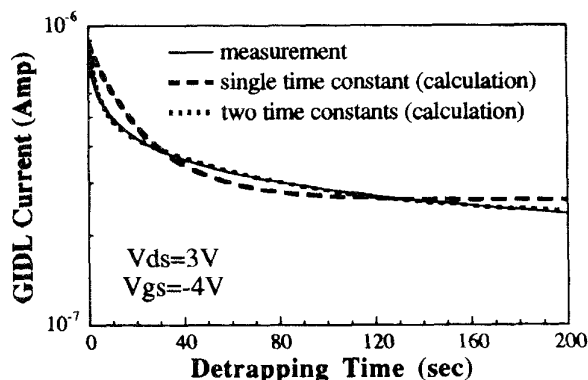


Fig. 4. Measured GIDL current transient and calculated results from (6). The dashed curve has one time-constant, $\tau_1 = 26.9$ and $\beta_1 = 1.22$. The dotted line has two time-constants, $\tau_1 = 4.5$ s, $\tau_2 = 79.4$ s, $\beta_1 = 0.57$ and $\beta_2 = 0.80$.

characteristics, we plot $\ln\left(\left|\frac{d}{dt}[\ln(I_d)]\right|\right)$ versus time in Fig. 3. The noise in the figure is associated with measurement and numerical differentiation. Apparently, this plot contains at least two different slopes (dashed lines). According to (8), these two linear slopes indicate the existence of two types of oxide traps with different detrapping time constants. The dispersion of the field-dependent detrapping time constant is believed due to nonuniform energetic or spatial distribution of the traps [7]. The result of an alternative time constant extraction procedure based on a least square error fit, which is much less sensitive to measurement noise, is shown in Fig. 4. Again, it was found that the measured GIDL transient (solid line) cannot be fitted well by a single time-constant model (dashed line) while a two time-constants model with $\tau_1 = 4.5$ s, $\tau_2 = 79.4$ s, $\beta_1 = 0.57$, and $\beta_2 = 0.80$ can reproduce the measured result excellently (dotted line). The multi-time-constant feature of oxide traps observed in this measurement is generally consistent with the findings by using flatband voltage measurement [6].

IV. CONCLUSION

We have proposed a new characterization technique to study the oxide trap transient characteristics. This technique has been shown to be very sensitive to an oxide charge variation. Using this method, we found that the hot electron stress generated oxide traps contain at least two distinct time constants.

REFERENCES

- [1] C. T. Wang, *Hot Carrier Design Considerations for MOS Devices and Circuits*. New York: Van Nostrand Reinhold, 1992.
- [2] C. Huang, T. Wang, T. Chen, N. C. Peng, A. Chang, and F. C. Shone, "Characterization and simulation of hot carrier effect on erasing gate current in flash EEPROM's," in *Proc. Int. Rel. Phys. Symp.*, 1995, pp. 61-64.
- [3] N. Matsukawa, S. Yamada, K. Amemiya, and H. Hazama, "A hot carrier induced low-level leakage current in thin silicon dioxide films," in *Proc. Int. Rel. Phys. Symp.*, 1995, pp. 162-167.
- [4] T. H. Ning, "Electron trapping in SiO₂ due to electron-beam deposition of aluminum," *J. Appl. Phys.*, vol. 49, pp. 4077-4082, 1978.
- [5] T. H. Ning and H. N. Yu, "Optically induced injection of hot electrons in SiO₂," *J. Appl. Phys.*, vol. 45, pp. 5373-5378, 1974.
- [6] R. F. De Keersmaecker, "Charge trapping in SiO₂," in *Insulating Films on Semiconductors*, J. F. Verweij and D. R. Wolters, Eds. Amsterdam, The Netherlands: Elsevier, 1983, pp. 85-97.
- [7] A. Balasinski, J. Worley, K. W. Huang, J. Walters, and F. T. Liou, "Observation of two types of trapping centers in thin film transistors using charge pumping technique," *IEEE Electron Device Lett.*, vol. 16, pp. 460-463, 1995.
- [8] Y. Nissan-Cohen, J. Shappir, and D. Frohman-Bentchkowsky, "Dynamic model of trapping-detrapping in SiO₂," *J. Appl. Phys.*, vol. 58, pp. 2252-2261, 1985.
- [9] J. F. Zhang, S. Taylor, and W. Eccleston, "Detrapping of trapped electrons in SiO₂ under Fowler-Nordheim stress," in *Insulating Films on Semiconductors 1991*. Liverpool, U.K.: Hilger, 1991, pp. 291-294.
- [10] T. Y. Chan, J. Chen, P. K. Ko, and C. Hu, "The impact of gate-induced drain leakage current on MOSFET scaling," *IEDM Tech. Dig.*, pp. 718-721, 1987.
- [11] B. Doyle, M. Bourcier, J. C. Maretaux, and A. Boudou, "Interface state generation and charge trapping in the medium-to-high gate voltage range ($V_d > V_g > 0.5V_d$) during hot carrier stressing of n-MOSFET's," *IEEE Trans. Electron. Devices*, vol. 37, pp. 744-754, 1990.
- [12] G. Q. Lo, D. L. Kwong, "Roles of oxide trapped charge and generated interface states in GIDL under hot carrier stressing," *IEDM Tech. Dig.*, pp. 557-560, 1990.
- [13] Z. J. Ma, P. T. Lai, and Y. C. Cheng, "Off-state instabilities in thermally nitrated-oxide n-MOSFET's," *IEEE Trans. Electron Devices*, vol. 40, pp. 125-130, 1993.